Open Access

ORIGINAL ARTICLE

Prostate Cancer

Mannose inhibits the growth of prostate cancer through a mitochondrial mechanism

Yu-Lin Deng[1,*], Ren Liu[1,*], Zhou-Da Cai[2], Zhao-Dong Han[3], Yuan-Fa Feng[4], Shang-Hua Cai[4], Qing-Biao Chen[6], Jian-Guo Zhu[5], Wei-De Zhong[1,3]

The limited treatment options for advanced prostate cancer (PCa) lead to the urgent need to discover new anticancer drugs. Mannose, an isomer of glucose, has been reported to have an anticancer effect on various tumors. However, the anticancer effect of mannose in PCa remains unclear. In this study, we demonstrated that mannose inhibits the proliferation and promotes the apoptosis of PCa cells *in vitro*, and mannose was observed to have an anticancer effect in mice without harming their health. Accumulation of intracellular mannose simultaneously decreased the mitochondrial membrane potential, increased mitochondrial and cellular reactive oxygen species (ROS) levels, and reduced adenosine triphosphate (ATP) production in PCa cells. Mannose treatment of PCa cells induced changes in mitochondrial morphology, caused dysregulated expression of the fission protein, such as fission, mitochondrial 1 (FIS1), and enhanced the expression of proapoptotic factors, such as BCL2-associated X (Bax) and BCL2-antagonist/killer 1 (Bak). Furthermore, lower expression of mannose phosphate isomerase (MPI), the key enzyme in mannose metabolism, indicated poorer prognosis in PCa patients, and downregulation of MPI expression in PCa cells enhanced the anticancer effect of mannose. This study reveals the anticancer effect of mannose in PCa and its clinical significance in PCa patients.

INTRODUCTION

Prostate cancer (PCa) is the most common malignancy and the second leading cause of cancer-related death in males.[1] Despite the benefits of androgen deprivation targeting androgen receptor (AR) signaling in the early stages of the disease, many tumors recur in an androgen-independent form, accompanied by an increased mortality rate. Therefore, identifying a more active and less toxic antitumor agent is a major goal in the development of new targeted therapeutic strategies.[2] Studies have demonstrated that tumorigenesis depends on the metabolic reprogramming that induces cancer cells to proliferate even under stress conditions.

Mannose is a natural monosaccharide and an isomer of glucose. Studies indicated that mannose can impair the growth of various tumors.[3,4] Mannose phosphate isomerase (MPI) is the key enzyme in mannose metabolism. The expression of MPI is related to the cellular content and the anticancer effect of mannose.[3] To date, the anticancer effect of mannose in PCa remains unclear. Here, we aim to investigate the anticancer effect of mannose in PCa and evaluate its possible application in PCa patients.

In this study, we found that mannose can inhibit the function of and induce morphological changes in mitochondria in PCa cells, thus inhibiting the growth and promoting the apoptosis of PCa cells.

Furthermore, we preliminarily verified that mannose may have better antitumor effects in PCa patients with worse pathological classification.

MATERIALS AND METHODS

Cell lines

The human PCa cell lines DU145 and PC3 were obtained from the American Type Culture Collection (ATCC® HTB-81 and ATCC® CRL1435, Manassas, VA, USA) and grown in Dulbecco's modified Eagle medium (DMEM; C11965500BT, Gibco, Paisley, UK) containing 10% fetal bovine serum, streptomycin, and penicillin. The normal human prostate epithelial cell line RWPE-1 was obtained from iCell (Shanghai, China) and grown in keratinocyte serum free medium (SFM; iCell-0019, iCell). Cells were incubated in a humidified, 5% CO_2 atmosphere at 37°C. The detailed information of reagents used in this study is shown in the **Supplementary Table 1**.

Measurement of the half-maximal inhibitory concentration (IC50) of mannose and cell proliferation assay

The IC50 of mannose (M2069, Sigma-Aldrich, Saint Louis, MO, USA) in PCa cells was determined and cell proliferation assays were conducted using a Cell Counting Kit-8 (CCK-8; CCK8-500T, Meilunbio, Dalian, China). For the IC50 assay, cells were plated in

[1]Guangdong Provincial Institute of Nephrology, Nanfang Hospital, Southern Medical University, Guangzhou 510515, China; [2]Department of Andrology, Guangzhou First People's Hospital, School of Medicine, South China University of Technology, Guangzhou 510180, China; [3]Department of Urology, Guangdong Key Laboratory of Clinical Molecular Medicine and Diagnostics, Guangzhou First People's Hospital, School of Medicine, South China University of Technology, Guangzhou 510180, China; [4]Urology Key Laboratory of Guangdong Province, The First Affiliated Hospital of Guangzhou Medical University, Guangzhou Medical University, Guangzhou 510230, China; [5]Department of Urology, Guizhou Provincial People's Hospital, The Affiliated Hospital of Guizhou Medical University, Guiyang 550002, China; [6]Department of Urology Surgery, Affiliated Foshan Hospital of Southern Medical University, Foshan 528000, China.
*These authors contributed equally to this article.
Correspondence: Dr. WD Zhong (zhongwd2009@live.cn) or Dr. JG Zhu (doctorzhujianguo@163.com)
Received: 11 June 2021; Accepted: 17 November 2021

96-well plates and cultured with multiple mannose concentrations for 72 h. The mannose concentrations in DMEM were 25 mmol l^{-1} and 50 mmol l^{-1} for DU145 and PC3, respectively, based on the IC50 values.

For cell proliferation, cells were plated in 96-well plates with a normal medium with or without mannose supplementation for 4–96 h. DMEM containing 10% CCK-8 was replaced in each well and incubated for another 2 h. The absorbance of the medium at a wavelength of 450 nm was determined using a microplate reader (Bio-Rad, Hercules, CA, USA).

Colony formation assay

Cells were plated in 6-well plates and maintained in medium with or without mannose supplementation, and replaced every 2 days, for a total of 10 days. Then, cells were fixed and stained with 0.1% crystal violet for 2 h. The siMPI-DU145 and siMPI-PC3 cells were retransfected every 72 h.

Apoptosis assay

Cells were plated in 6-well plates, cultured in medium with or without mannose for 48 h, and resuspended in binding buffer. Then, cells were stained with Annexin V-fluorescein isothiocyanate (FITC) and propidium iodide (PI) containing RNase A (AP105, MultiSciences, Hangzhou, China). After staining, cells were harvested and subjected to a flow cytometer (BD FACSVerse, BD Biosciences, Franklin Lakes, NJ, USA). FlowJo software (BD Biosciences) was used to analyze the data.

Xenograft model

Four-week-old male nude mice (Experimental Animal Center of Sun Yat-sen University, Guangzhou, China) were raised under specific pathogen-free conditions. Animal handling and protocols were approved by the Institutional Animal Care and Use Committee of Guangzhou Medical University (Guangzhou, China) according to the National Research Council's guidelines. The certificate number of the animal breeder was 2018217474. A total of 5×10^6 DU145 cells were injected subcutaneously. Mice were randomly divided into the control group and mannose group (5 mice per group). Mice received mannose (20%) by oral gavage (200 μl) every 2 days starting on the 12th day. The mouse weight and tumor volume (length [mm] × width^2 [mm^2] × 1/2) were measured every 2 days. When the mice were euthanized, the tumors and organs (*i.e.*, liver, kidney, and pancreas) were harvested to identify the effect of mannose on mouse health. The effect of mannose on the growth of PCa tumors *in vivo* was determined by the formula (tumor final volume [mm^3] – initial volume [mm^3]).

5,5',6,6'-tetrachloro-1,1',3,3'-tetraethyl-imidacarbocyanine (JC-1) staining

The mitochondrial membrane potential (MMP) was evaluated by JC-1 staining (M8650, Solarbio, Beijing, China). Cells were plated in 6-well plates and cultured in medium with or without mannose for 48 h. Cells were incubated for 30 min for mitochondrial staining with JC-1, and nuclei were then stained with Hoechst 33342 (100 nmol l^{-1}; C1028, Beyotime, Shanghai, China) for 10 min. After staining, cells were observed under a confocal microscope (LSM880, Zeiss, Jena, Germany). JC-1 aggregates (red fluorescence) indicate a normal MMP, while JC-1 monomers (green fluorescence) indicate a decreased MMP.

Rhodamine 123 staining

The MMP was also measured by rhodamine 123 staining (HY-D8016, MCE, Monmouth Junction, NJ, USA). Cells were cultured in the same way as JC-1 staining and incubated with rhodamine 123 (200 ng ml^{-1}) for 30 min. Cells were harvested and subjected to BD FACSVerse. FlowJo software was used to calculate the mean fluorescence intensity (MFI) of each sample. The rhodamine 123 MFI increases when the MMP decreases.

Quantification of mitochondrial and cellular reactive oxygen species (ROS)

Cells were cultured in the same way as JC-1 staining and incubated with MitoSOX red (5 μmol l^{-1}; M36008, Invitrogen, Waltham, MA, USA) or DCFH-DA (10 μmol l^{-1}; D6883, Sigma-Aldrich) for 30 min. Cells were harvested and subjected to BD FACSVerse. FlowJo software was used to calculate the MFI of each sample.

Measurement of adenosine triphosphate (ATP) generation

The ATP content was measured with an Enhanced ATP Assay Kit (S0027, Beyotime). Cells were cultured in the same way as JC-1 staining. Tumors were harvested from xenograft model mice. Cells were harvested and centrifuged at 12 000g and 4°C for 5 min by high speed refrigerated centrifuge (Sorvall Legend Micro 17R, ThermoFisher, Waltham, MA, USA). Then, 100 μl of ATP detection solution and 20 μl of the cell supernatant were added to a 96-well plate, and ATP was detected using a multifunctional microplate reader (Varioskan LUX, ThermoFisher). ATP content was calculated according to the standard curve.

MitoTracker staining

Cells were cultured in the same way as JC-1 staining. Mitochondria in PCa cells were stained with MitoTracker Red CMXRos (100 nmol l^{-1}; C1049, Beyotime) for 30 min. Then, cells were observed under a confocal microscope (LSM880, Zeiss).

Transmission electron microscopy

Cells were cultured in the same way as JC-1 staining. The protocols were performed, as previously described.[5] Quantification of the mitochondrial volume was performed by first drawing a contour of the cross-section of each mitochondrion and then calculating the enclosed area in ImageJ software (National Institutes of Health, Bethesda, MD, USA).

Western blot analysis

Protein extraction and western blot analysis were performed, as previously described.[6] The following antibodies were used at a dilution of 1:1000 unless otherwise stated: rabbit anti-MPI (ab154198, Abcam, Cambridge, UK), rabbit anti-mitofusin 1 (MFN1; 13798-1-AP, Proteintech, Chicago, IL, USA), rabbit anti-MFN2 (12186-1-AP, Proteintech), rabbit anti-fission, mitochondrial 1 (FIS1; 10956-1-AP, Proteintech), rabbit anti-dynamin related protein 1 (DRP1; 26187-1-AP, Proteintech), rabbit anti-BCL2-associated X (Bax; 9942T, CST, Boston, MA, USA), rabbit anti-BCL2-antagonist/killer 1 (Bak; 9942T, CST), mouse anti-β-actin (1:5000; ab8227, Abcam), and mouse anti-glyceraldehyde-3-phosphate dehydrogenase (GAPDH; 1:10 000; 60004-1-AP, Proteintech).

Measurement of mannose concentration

PCa cells were cultured in the same way as JC-1 staining and harvested. Tumors were harvested from xenograft model mice. The assay was performed with a Human Mannose ELISA Kit (ZK-H594, ZIKER, Shenzhen, China) following the manufacturer's instructions, and the optical density was measured at a 450 nm wavelength using a multifunctional microplate reader. Mannose concentrations were calculated according to the standard curve.

Patients and tissues

A PCa tissue microarray (TMA; PR803d, Biomax, Derwood, MD, USA) was applied for immunohistochemical analysis. Patients did

not receive chemotherapy or radiotherapy before surgery. Detailed information on the TMA cohort is available in the supplementary materials. PCa tissues and paired clinical data were collected from 498 patients with information in the TCGA database (TCGA-PRAD, The Cancer Genome Atlas-Prostate Adenocarcinoma: https://www.cancer.gov/tcga), and correlations between the MPI mRNA expression level and patients' clinicopathological features were assessed. This study was approved by the Ethics Committee of Guangzhou First People's Hospital (approval No. 82072813).

Immunohistochemistry (IHC)
MPI protein expression in our TMA cohort was assessed by IHC, as previously described.[7] An IHC kit (KIT-9730, MXB, Fuzhou, China) and rabbit anti-MPI antibody (1:400; ab154198, Abcam) were used for immunostaining following the manufacturer's instructions.

Overexpression of FIS1 in PCa cells
PCa cells were transfected with pcDNA-FIS1 or pcDNA (GenePharma, Shanghai, China) using Lipofectamine 3000 (L3000008, Invitrogen, Waltham, MA, USA) for 72 h. After transfection, cells were collected.

Silencing of MPI using small interfering RNA (siRNA)
PCa cells were transfected with human MPI siRNA or control siRNA (GenePharma, Shanghai, China) using GP-transfect-Mate (GenePharma) for 72 h. Cells were collected, and silencing was confirmed by western blot.

Statistical analyses
All of the statistical analyses were performed with SPSS Statistics 20 (IBM, New York, NY, USA) and GraphPad Prism 8 (GraphPad Software, San Diego, CA, USA). Continuous variables were expressed as means ± standard deviation (s.d.). Student's *t*-test or analysis of variance (ANOVA) was used to determine the statistical significance of our quantitative data. The Kaplan–Meier method was used for survival analysis. The optimal cutoff value was determined using the R package "survminer". Differences with $P < 0.05$ were considered to be statistically significant.

RESULTS

Effect of mannose on the growth of PCa cells in vitro
The IC50 values of mannose were 67.42 mmol l^{-1} (95% confidence interval [CI]: 57.680–78.960) and 177.00 mmol l^{-1} (95% CI: 166.800–188.000) in DU145 and PC3 cells, respectively (**Figure 1a** and **1b**). After mannose treatment, the intracellular mannose concentrations increased in PCa cells ($P < 0.01$; **Figure 1c**). The inhibitory effects of mannose on DU145 and PC3 were observed in the growth curve 72 h after mannose treatment (DU145: $P < 0.01$, and PC3: $P < 0.05$; **Figure 1d** and **1e**). Mannose reduced the number of colonies ($P < 0.01$; **Figure 1f** and **1g**) of PCa cells. The apoptosis rate increased after mannose treatment (DU145: $P < 0.05$, and PC3: $P < 0.01$; **Figure 1h** and **1i**). Mannose had no effect on the growth or colony formation of RWPE-1 (**Supplementary Figure 1a** and **1b**).

Effect of mannose on the growth of PCa cells in vivo
In the xenograft tumor assay, five nude mice per group received a subcutaneous injection of DU145 cells. However, the xenograft tumor in one nude mouse did not grow after mannose treatment. Therefore, the volume of this tumor was not included in our statistical analysis. Our results showed that oral mannose administration inhibited PCa tumor growth in nude mice ($P < 0.01$; **Figure 2a–2d**), while oral administration of mannose had no effect on body weight (**Figure 2g**) or the weights of the liver, kidney, and pancreas (**Figure 2h**) in mice.

Intratumoral mannose concentration increased ($P < 0.01$; **Figure 2e**) and the ATP content decreased ($P < 0.01$; **Figure 2f**) in the mannose group.

Mannose disrupted mitochondrial function, led to ROS overproduction, and activated Bax/Bak in PCa cells
JC-1 staining showed an increase in JC-1 monomers and a decrease in JC-1 aggregates after mannose treatment (**Figure 3a**), suggesting a reduction in the MMP. The rhodamine 123 assay showed a decreased MMP in PCa cells treated with mannose ($P < 0.01$; **Figure 3b**), consistent with the results of JC-1 staining. Mannose decreased the ATP content in PCa cells ($P < 0.01$; **Figure 3c**) but had no effect in RWPE-1 (**Supplementary Figure 1c**). Mannose increased both the mitochondrial ($P < 0.01$; **Figure 3d**) and cellular ($P < 0.01$; **Figure 3e**) ROS levels. Western blot analysis (**Figure 3f**) indicated that the expression of Bax (DU145: $P < 0.05$, and PC3: $P < 0.01$; **Figure 3g**) and Bak ($P < 0.01$; **Figure 3g**) was enhanced in PCa cells after mannose treatment.

Mannose disrupted the balance of mitochondrial dynamics in PCa cells
Confocal microscopy revealed that mannose treatment resulted in the elongation of mitochondria in PCa cells (**Figure 4a**). Transmission electron microscopy was used to further observe the structure of mitochondria and showed an increase in the mitochondrial cross-sectional area with mannose treatment ($P < 0.01$; **Figure 4b**).

Western blot analysis (**Figure 4c**) indicated that the expression of the mitochondrial fission protein FIS1 decreased in PCa cells (DU145: $P < 0.01$ and PC3: $P < 0.05$; **Figure 4c**). Cellular ATP content increased ($P < 0.01$; **Figure 4e**), while FIS1 overexpressed in PCa cells ($P < 0.01$; **Figure 4d**). No changes in MFN1, MFN2, or DRP1 expression were observed with mannose treatment (**Supplementary Figure 2a** and **2b**).

Downregulated MPI expression enhanced the anticancer effect of mannose on PCa cells
MPI was silenced in PCa cells ($P < 0.01$; **Figure 5a** and **5b**). After silencing MPI, the intracellular mannose concentration increased ($P < 0.01$; **Figure 5c**) and the ATP content decreased ($P < 0.01$; **Figure 5d**) with mannose treatment. The growth curves showed that in MPI-downregulated cells, the anticancer effect of mannose was more obvious within 48 h in DU145 and appeared after 72 h in PC3 ($P < 0.05$; **Figure 5e**). In addition, mannose treatment more obviously reduced the number of colonies of MPI-downregulated PCa cells ($P < 0.01$; **Figure 5f**).

MPI protein and mRNA expression in human PCa tissues
The expression of MPI in PCa tissues was investigated by IHC (**Supplementary Figure 3**). The mean IRS of MPI expression in PCa of GS ≥ 8 and GS ≤ 7 was 7.563 and 10.000 in the TMA chort, respectively. ($P = 0.003$; **Figure 5g**). In addition, the results of The Cancer Genome Atlas Prostate Adenocarcinoma (TCGA-PRAD) analysis indicated that the mean *MPI* mRNA expression levels in PCa tissues of GS ≥ 8 and GS ≤ 7 were 5.995 and 6.278, respectively ($P < 0.001$; **Table 1**).

Reduced MPI expression is associated with aggressive progression and poor prognosis of PCa
The associations between MPI expression and clinicopathological characteristics of PCa patients based on our TMA data and TCGA-PRAD database analysis are shown in **Table 1**. Low MPI expression in PCa tissues was associated with high Gleason scores (IHC data: $P = 0.003$, TCGA-PRAD database: $P < 0.001$), advanced
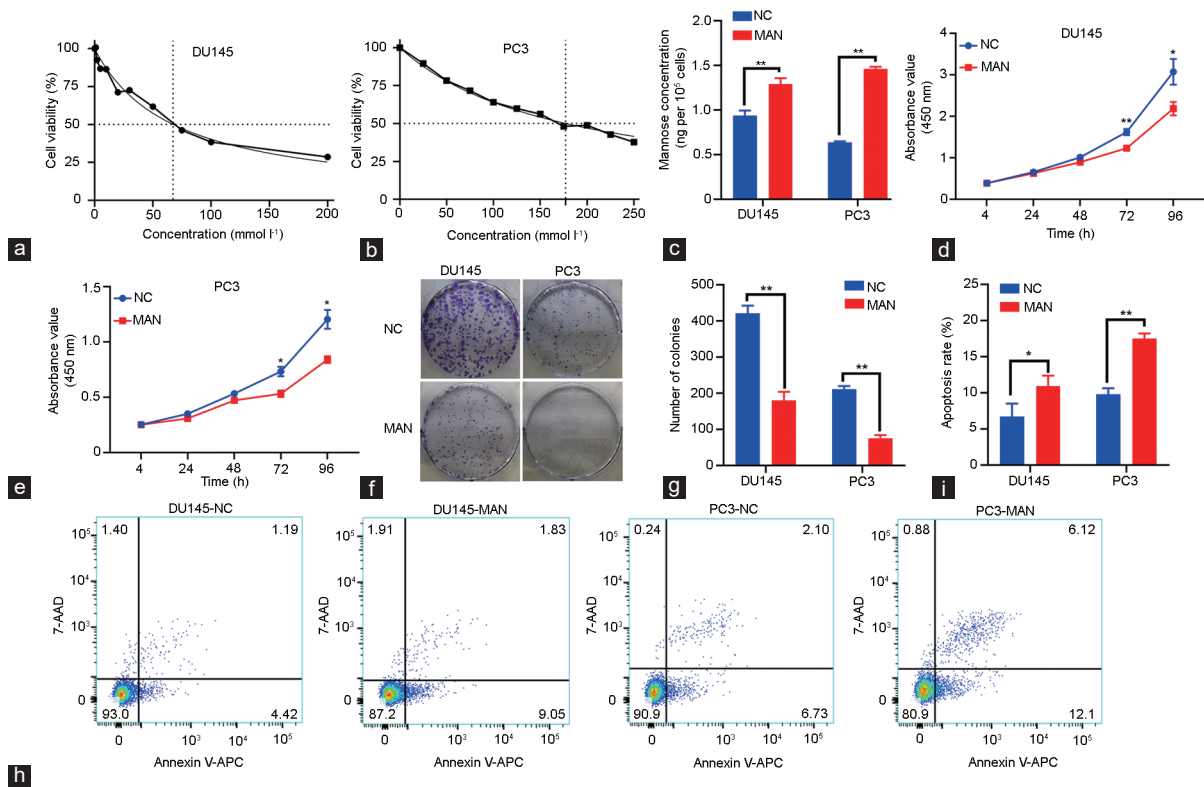
Figure 1: Mannose inhibited the proliferation and induced the apoptosis of PCa cells. The IC50 of mannose in (**a**) DU145 and (**b**) PC3 cells was determined using a CCK-8 assay. (**c**) Intracellular mannose concentration in PCa cells. Cell proliferation of (**d**) DU145 and (**e**) PC3 was assessed using growth curves, respectively. (**f**) Colony formation assays were performed and (**g**) colony numbers were counted in PCa cells. (**h**) Flow cytometric analysis was used to assess (**i**) the apoptosis rate of PCa cells. $^*P < 0.05$, $^{**}P < 0.01$. NC: PCa cells cultured in normal medium. MAN: PCa cells cultured in normal medium with 25 mmol l^{-1} mannose for DU145 or with 50 mmol l^{-1} mannose for PC3. PCa: prostate cancer; IC50: the half-maximal inhibitory concentration; CCK-8: Cell Counting Kit-8 ; AAD: Aminoactinomycin D; APC: Allophycocyanin.
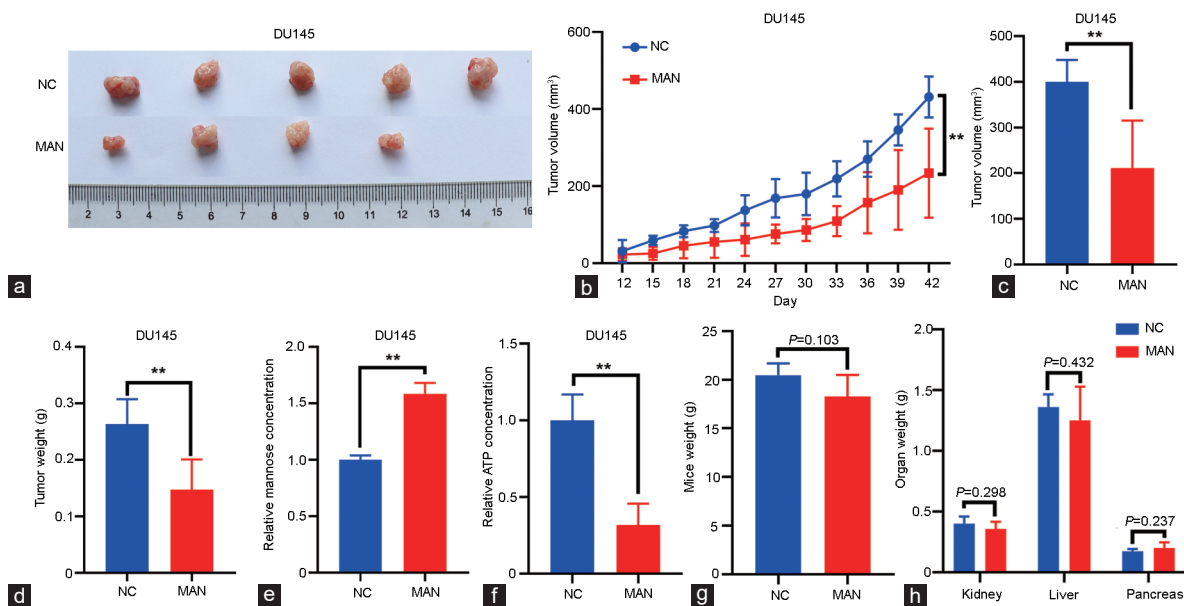
Figure 2: Mannose inhibited tumor growth in a PCa xenograft model without affecting mice health. (**a**) Subcutaneous tumors from the xenograft model with DU145 cells. (**b**) Tumor growth was monitored for 30 days after mannose treatment. (**c**) The volume of tumor growth. (**d**) The weight of the tumors. (**e**) Intratumoral mannose concentration and (**f**) ATP content in subcutaneous tumors. The weights of (**g**) mice and (**h**) major metabolic organs. $^{**}P < 0.01$. NC: PCa cells cultured in normal medium. MAN: PCa cells cultured in normal medium with 25 mmol l^{-1} mannose for DU145 or with 50 mmol l^{-1} mannose for PC3. PCa: prostate cancer; ATP: adenosine triphosphate.
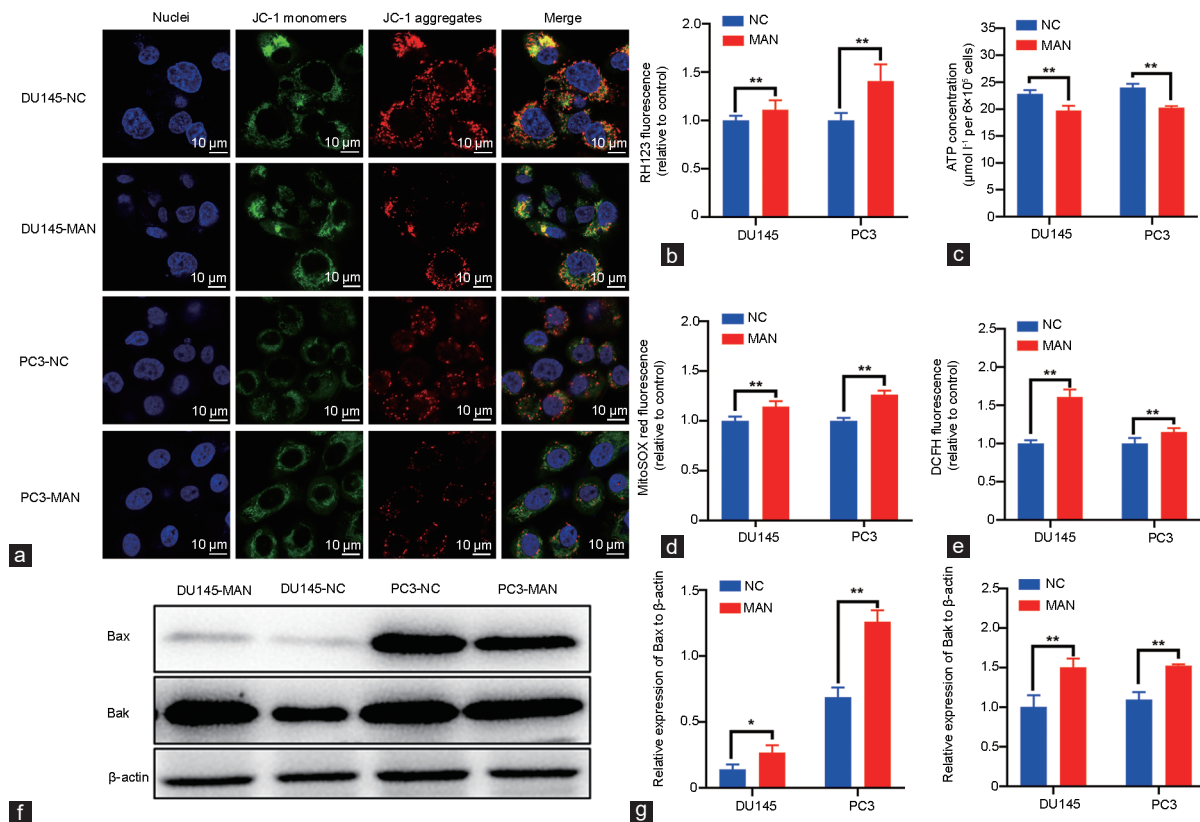
Figure 3: Mannose disrupted mitochondrial function, led to ROS overproduction, and activated Bax/Bak in PCa cells. (**a**) JC-1 staining and (**b**) rhodamine 123 staining were used to assess the MMP in DU145 and PC3 cells. (**c**) The ATP content in cells. (**d**) Mitochondrial ROS and (**e**) cellular ROS levels in cells. (**f** and **g**) The protein expression of Bax and Bak in cells. $^*P < 0.05$, $^{**}P < 0.01$. NC: PCa cells cultured in normal medium. MAN: PCa cells cultured in normal medium with 25 mmol l^{-1} mannose for DU145 or with 50 mmol l^{-1} mannose for PC3. JC-1: 5,5′,6,6′-tetrachloro-1,1′,3,3′-tetraethyl-imidacarbocyanine; Bax: BCL2-associated X; Bak: BCL2-antagonist/killer 1; ROS: reactive oxygen species; MMP: mitochondrial membrane potential; ATP: adenosine triphosphate; PCa: prostate cancer.

pathological stage (TCGA-PRAD database: $P < 0.001$), and positive metastasis (TCGA-PRAD database: $P < 0.001$).

Survival analysis was performed using the TCGA-PRAD database. Patients were stratified into a high-expression group and a low-expression group based on the optimal cutoff value (cutoff value = 5.940; **Supplementary Figure 4a**) for MPI expression. Kaplan–Meier analysis showed that patients in the low-expression group had significantly worse BCR outcomes than those in the high-expression group (HR = 0.455, 95% CI: 0.250–0.830, $P = 0.003$; **Figure 5h**). Kaplan–Meier analysis also suggested that there was no statistically significant difference in OS between the high-expression and low-expression groups (HR = 0.411, 95% CI: 0.110–1.610, $P = 0.144$; **Figure 5i**) using the optimal cutoff value (cutoff value: 6.000; **Supplementary Figure 4b**).

DISCUSSION

Most PCa patients develop androgen resistance accompanied by poor therapeutic effects; thus, a new potential therapy is urgently needed. Metabolic reprogramming is a major hallmark of cancer. In normal prostatic peripheral zone epithelial cells, the tricarboxylic acid (TCA) cycle is halted in mitochondria.[8] PCa cells reversed this phenotype and the TCA cycle is activated.[9]

Mannose has shown potential therapeutic properties in a variety of cancers.[10–12] We found that mannose can inhibit the growth of PCa cells. Furthermore, mannose can regulate metabolic reprogramming

of osteosarcoma cells.[3,13] Similar to these results, we found mannose-induced metabolic changes in PCa cells. After mannose treatment, decreased mitochondrial membrane potential indicated mitochondrial dysfunction, resulting in a decrease in ATP production, suggesting that mannose inhibits mitochondrial ATP production in PCa cells.

Accumulated intracellular mannose inhibits the growth of osteosarcoma and enhances the chemotherapeutic effect of doxorubicin.[3] We found that mannose accumulated in PCa cells and tumors treated with mannose. Furthermore, silencing MPI increased the intracellular mannose concentration and enhanced the anticancer effect of mannose on PCa, consistent with a previous study.[3] These results suggest that MPI plays a role in promoting intracellular accumulation of mannose, thus inhibiting PCa cell proliferation.

ROS are mainly produced when mitochondria consume oxygen.[14] ROS are toxic to cancer cells when ROS production exceeds the ROS scavenging ability.[15] Aberrant elevated ROS can be achieved with cytotoxic stimulation, and we observed that after mannose treatment, the mitochondrial and cellular ROS levels in PCa cells significantly increased, while the growth of PCa cells was inhibited and their apoptosis was promoted. These results suggest that intracellular accumulation of mannose can lead to excessive production of ROS and toxic effects on PCa cells. Overproduction of ROS may also affect the activity of apoptotic effectors.[16] Bax and Bak are proapoptotic proteins that play a core role in mitochondrial membrane permeabilization and apoptotic signaling.[17] Upon cytotoxic stress, Bax and Bak disrupt the
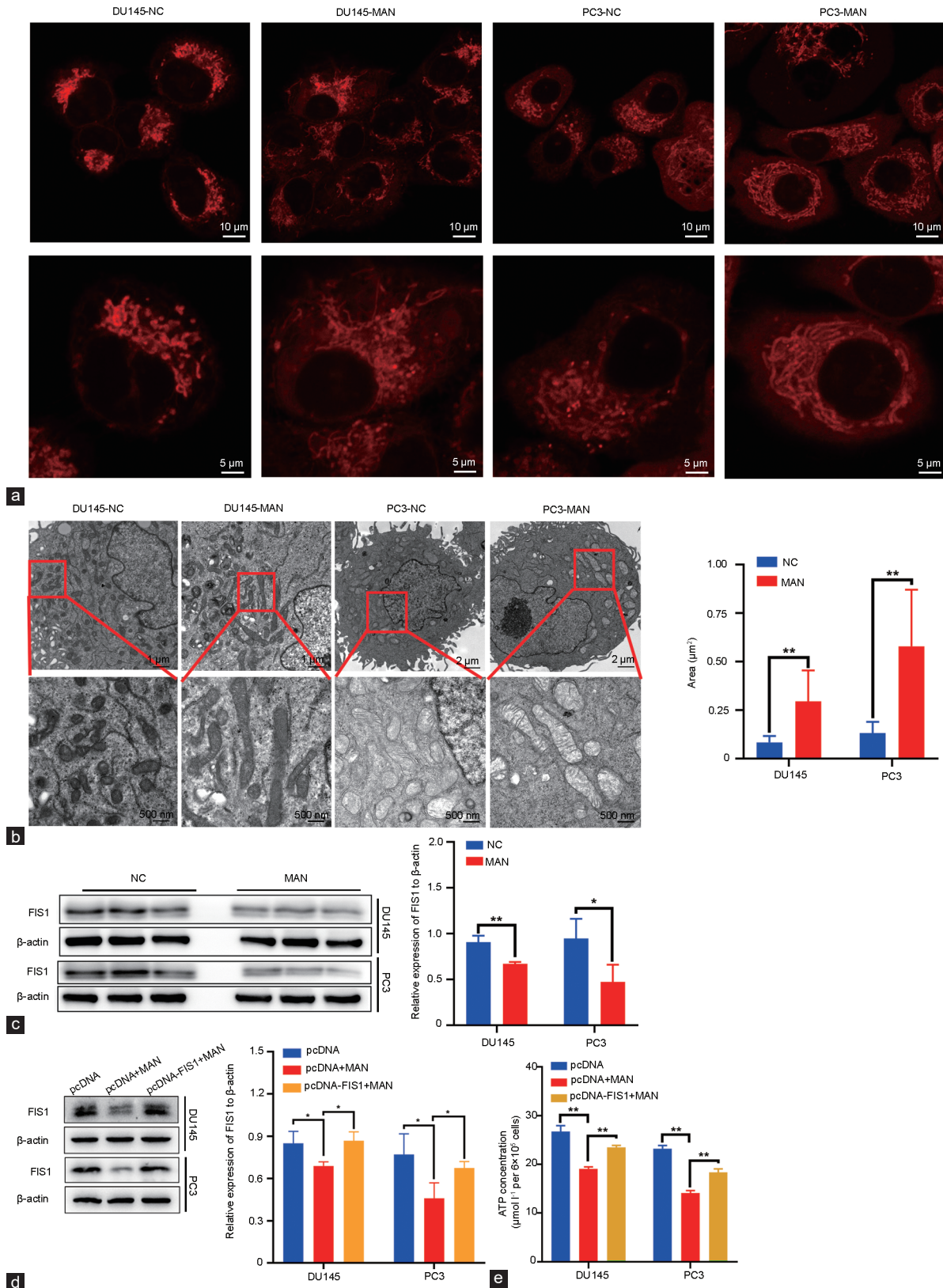
Figure 4: Mannose disrupted the balance of mitochondrial dynamics in PCa cells. (**a**) Mitochondria stained with MitoTracker Red were observed by confocal microscopy. (**b**) Mitochondrial structure under a transmission electron microscopy, and the mitochondrial cross-sectional area was quantified. (**c**) The protein expression of FIS1 in cells. Upregulated (**d**) FIS1 and (**e**) increased ATP content in PCa cells. $^*P < 0.05$, $^{**}P < 0.01$. NC: PCa cells cultured in normal medium. MAN: PCa cells cultured in normal medium with 25 mmol l^{-1} mannose for DU145 or with 50 mmol l^{-1} mannose for PC3. ATP: adenosine triphosphate; FIS1: fission, mitochondrial 1; PCa: prostate cancer.
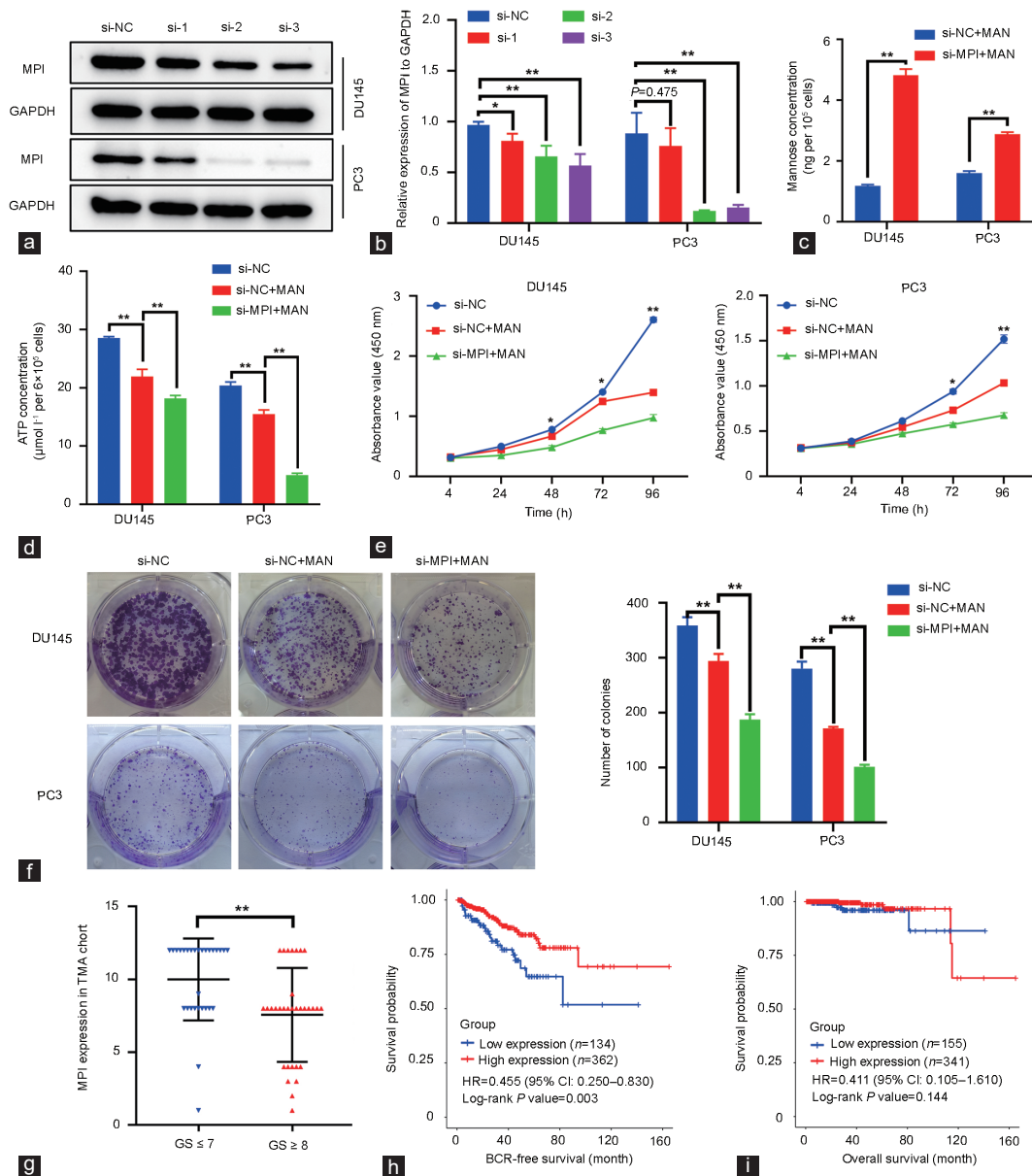
Figure 5: Downregulation of MPI expression enhances the anticancer effect of mannose. The expression of MPI in human prostate cancer tissues and its prognostic value. (**a** and **b**) The expression of MPI was silenced by siRNA-MPI and verified by western blotting. siRNA-MPI with different base sequences including si-1, si-2 and si-3 were used for downregulating the MPI expression in PCa cells. According to the degree of down-regulation of MPI protein, si-3 and si-2 with the best interference effect were applied to DU145 and PC3 cells, respectively. (**c**) Intracellular mannose concentration and (**d**) ATP content in cells. (**e**) Growth curves and (**f**) colony formation assays of cells. (**g**) The IHC scores for MPI expression in PCa tissues. (**h**) Kaplan–Meier curves of BCR-free survival and (**i**) overall survival for the low and high MPI expression groups of patients in the TCGA-PRAD dataset. $^*P < 0.05$, $^{**}P < 0.01$. NC: PCa cells cultured in normal medium. MAN: PCa cells cultured in normal medium with 25 mmol l^{-1} mannose for DU145 or with 50 mmol l^{-1} mannose for PC3. MPI: mannose phosphate isomerase; si: siRNA, small interfering RNA; IHC: immunohistochemistry; PCa: prostate cancer; BCR: biochemical recurrence; TCGA-PRAD: The Cancer Genome Atlas-Prostate Adenocarcinoma; GAPDH: glyceraldehyde-3-phosphate dehydrogenase; TMA: tissue microarray; ATP: adenosine triphosphate.

mitochondrial outer membrane to allow the release of proapoptotic factors into the cytosol,[18] thus inducing the apoptosis of cells. We found upregulated expression of Bax and Bak and increased apoptosis in PCa cells under mannose treatment, suggesting that mannose induced apoptosis in PCa cells via the proapoptotic signaling of Bax and Bak.

Mitochondria are highly dynamic organelles, and their morphology is determined by mitochondrial dynamics through the interplay of fusion and fission. The main mediator of mitochondrial fission is DRP1,[19] which is recruited from the cytoplasm by FIS1[20]

and then induces mitochondrial division.[21] Cellular metabolic state can affect the balance of mitochondrial dynamics.[22] Changes in mitochondrial dynamics-related proteins are accompanied by cellular metabolic changes and have been observed in bladder cancer cells.[23] It was shown that miR-483-5p controls mitochondrial fission by targeting FIS1.[24] Deletion of FIS1 can lead to the elongation and swelling of mitochondria.[25] After mannose stimulation, the mitochondrial morphology became increasingly swollen and elongated along with the downregulation of FIS1. Besides, the

Table 1: Association of mannose phosphate isomerase expression with clinicopathological characteristics of patients with prostate cancer in the TMA and TCGA-PRAD

Clinical feature	MPI expression in the PCa TMA			MPI expression in TCGA-PRAD dataset		
	n	Mean±s.d.	P	n	Mean±s.d.	P
MPI expression			0.135			<0.001
Benign	12	10.170±2.329		52	2.817±0.295	
Cancer	62	8.677±3.243		494	3.192±0.346	
Age (year)			0.125			0.017
<65	19	9.632±3.419		328	6.196±0.428	
≥65	43	8.256±3.110		166	6.092±0.501	
Gleason score*			0.003			<0.001
≤7	29	10.000±2.816		290	6.278±0.398	
≥8	32	7.563±3.222		204	5.995±0.482	
Pathological stage			0.899			<0.001
<T3a	39	8.718±3.095		186	6.284±0.388	
≥T3a	23	8.609±3.551		301	6.090±0.480	
Metastasis			0.606			<0.001
No	56	8.607±3.262		317	6.197±0.422	
Yes	6	9.333±3.266		80	5.899±0.520	
Overall survival			-			0.860
Alive	-	-		484	6.162±0.457	
Dead	-	-		10	6.136±0.409	
PSA failure			-			0.078
Negative	-	-		91	6.085±0.510	
Positive	-	-		397	6.179±0.443	

*One sample of prostate adenocarcinoma tissue had no Gleason score. -: lack of relative information of patients in the cohort; MPI: mannose phosphate isomerase; PCa: prostate cancer; TMA: tissue microarray; TCGA-PRAD: The Cancer Genome Atlas-Prostate Adenocarcinoma; s.d.: standard deviation; PSA: prostate-specific antigen

ATP content increased in FIS1-overexpressing PCa cells under mannose treatment. Therefore, we considered that these changes in mitochondria were due to the downregulation of FIS1, which led to dysregulation of mitochondrial division under mannose treatment, although the mechanism has yet to be determined. Studies suggest that inhibiting the fission of mitochondria can inhibit the growth of cancer cells.[26] In contrast, increasing mitochondrial fission can inhibit mitochondria-dependent apoptosis, promote the proliferation of liver cancer cells,[27] and promote the migration and invasion of breast cancer cells.[28] The role of mitochondrial fission in apoptosis is still controversial;[29,30] however, it is widely believed that dynamin related protein 1 (DRP1) is not required for activation of Bax and Bak.[31,32] In addition, we observed increased apoptosis of PCa cells without DRP1 upregulation under mannose treatment, consistent with previous findings.

Consistent with the results of a relevant study on osteosarcoma,[3] silencing MPI expression enhanced the anticancer effect of mannose on PCa. Moreover, our analysis indicated that low MPI expression in PCa tissues was associated with high Gleason scores, advanced pathological classification, and poor clinical prognosis of PCa patients. This suggests that mannose may have an important potential therapeutic effect in advanced PCa patients.

In summary, our findings demonstrate that mannose can effectively inhibit the growth and promote the apoptosis of PCa cells through a change in mitochondrial function and morphology and a ROS-activated Bax- and Bak-dependent mitochondrial mechanism. Long-term oral mannose administration can inhibit the growth of PCa cells in nude mice without affecting their health. Moreover, MPI has important prognostic significance in PCa patients. Silencing MPI can increase the intracellular mannose concentration and enhance the anticancer effect of mannose in PCa. Thus, mannose may be used as a potential therapeutic agent for PCa.

AUTHOR CONTRIBUTIONS

YLD performed the cellular studies and the statistical analysis. RL performed the IHC assays and the statistical analysis. ZDC performed the xenograft model studies and the statistical analysis. YLD, RL, and ZDC participated in drafting the manuscript. ZDH and YFF performed the bioinformatic analysis. SHC and QBC participated in the cellular studies. WDZ and JGZ conceived of the study, participated in its design and coordination, and helped to revise the manuscript. All authors read and approved the final manuscript.

COMPETING INTERESTS

All authors declare no competing financial interests.

ACKNOWLEDGMENTS

Supplementary Information is linked to the online version of the paper on the *Asian Journal of Andrology* website.

REFERENCES

1   Siegel RL, Miller KD, Fuchs HE, Jemal A. Cancer statistics, 2021. *CA Cancer J Clin* 2021; 71: 7–33.
2   Cattaruzza L, Fregona D, Mongiat M, Ronconi L, Fassina A, *et al*. Antitumor activity of gold(III)-dithiocarbamato derivatives on prostate cancer cells and xenografts. *Int J Cancer* 2011; 128: 206–15.
3   Gonzalez PS, O'Prey J, Cardaci S, Barthet VJ, Sakamaki JI, *et al*. Mannose impairs

tumour growth and enhances chemotherapy. *Nature* 2018; 563: 719–23.

4   Luo Q, Li B, Li G. Mannose suppresses the proliferation and metastasis of lung cancer by targeting the ERK/GSK-3β/β-catenin/SNAIL axis. *Onco Targets Ther* 2020; 13: 2771–81.

5   Lu J, Dong W, He H, Han Z, Zhuo Y, *et al*. Autophagy induced by overexpression of DCTPP1 promotes tumor progression and predicts poor clinical outcome in prostate cancer. *Int J Biol Macromol* 2018; 118: 599–609.

6   Xie J, Ye J, Cai Z, Luo Y, Zhu X, *et al*. GPD1 enhances the anticancer effects of metformin by synergistically increasing total cellular glycerol-3-phosphate. *Cancer Res* 2020; 80: 2150–62.

7   Cai C, Chen QB, Han ZD, Zhang YQ, He HC, *et al*. miR-195 inhibits tumor progression by targeting RPS6KB1 in human prostate cancer. *Clin Cancer Res* 2015; 21: 4922–34.

8   Costello LC, Feng P, Milon B, Tan M, Franklin RB. Role of zinc in the pathogenesis and treatment of prostate cancer: critical issues to resolve. *Prostate Cancer Prostatic Dis* 2004; 7: 111–7.

9   Franz MC, Anderle P, Bürzle M, Suzuki Y, Freeman MR, *et al*. Zinc transporters in prostate cancer. *Mol Aspects Med* 2013; 34: 735–41.

10   Sha J, Cao D, Cui R, Xia L, Hua X, *et al*. Mannose impairs lung adenocarcinoma growth and enhances the sensitivity of A549 cells to carboplatin. *Cancer Manag Res* 2020; 12: 11077–83.

11   Wang Y, Xie S, He B. Mannose shows antitumour properties against lung cancer via inhibiting proliferation, promoting cisplatin mediated apoptosis and reducing metastasis. *Mol Med Rep* 2020; 22: 2957–65.

12   Liu F, Xu X, Li C, Li C, Li Y, *et al*. Mannose synergizes with chemoradiotherapy to cure cancer via metabolically targeting HIF-1 in a novel triple-negative glioblastoma mouse model. *Clin Transl Med* 2020; 10: e226.

13   Fang Z, Wang R, Zhao H, Yao H, Ouyang J, *et al*. Mannose promotes metabolic discrimination of osteosarcoma cells at single-cell level by mass spectrometry. *Anal Chem* 2020; 92: 2690–6.

14   Handy DE, Loscalzo J. Redox regulation of mitochondrial function. *Antioxid Redox Signal* 2012; 16: 1323–67.

15   Moon DO, Kim MO, Choi YH, Hyun JW, Chang WY, *et al*. Butein induces G(2)/M phase arrest and apoptosis in human hepatoma cancer cells through ROS generation. *Cancer Lett* 2010; 288: 204–13.

16   Groeger G, Quiney C, Cotter TG. Hydrogen peroxide as a cell-survival signaling molecule. *Antioxid Redox Signal* 2009; 11: 2655–71.

17   Kelekar A, Thompson CB. Bcl-2-family proteins: the role of the BH3 domain in apoptosis. *Trends Cell Biol* 1998; 8: 324–30.

18   Gilbert RJ, Dalla Serra M, Froelich CJ, Wallace MI, Anderluh G. Membrane pore formation at protein-lipid interfaces. *Trends Biochem Sci* 2014; 39: 510–6.

19   Pagliuso A, Cossart P, Stavru F. The ever-growing complexity of the mitochondrial fission machinery. *Cell Mol Life Sci* 2018; 75: 355–74.

20   Hoppins S, Nunnari J. Cell biology. Mitochondrial dynamics and apoptosis – the ER connection. *Science* 2012; 337: 1052–4.

21   Chen H, Detmer SA, Ewald AJ, Griffin EE, Fraser SE, *et al*. Mitofusins Mfn1 and Mfn2 coordinately regulate mitochondrial fusion and are essential for embryonic development. *J Cell Biol* 2003; 160: 189–200.

22   Dietrich MO, Liu ZW, Horvath TL. Mitochondrial dynamics controlled by mitofusins regulate Agrp neuronal activity and diet-induced obesity. *Cell* 2013; 155: 188–99.

23   Konstantakou EG, Voutsinas GE, Velentzas AD, Basogianni AS, Paronis E, *et al*. 3-BrPA eliminates human bladder cancer cells with highly oncogenic signatures via engagement of specific death programs and perturbation of multiple signaling and metabolic determinants. *Mol Cancer* 2015; 14: 135.

24   Fan S, Chen WX, Lv XB, Tang QL, Sun LJ, *et al*. miR-483-5p determines mitochondrial fission and cisplatin sensitivity in tongue squamous cell carcinoma by targeting FIS1. *Cancer Lett* 2015; 362: 183–91.

25   Pei S, Minhajuddin M, Adane B, Khan N, Stevens BM, *et al*. AMPK/FIS1-mediated mitophagy is required for self-renewal of human AML stem cells. *Cell Stem Cell* 2018; 23: 86–100.e6.

26   Rehman J, Zhang HJ, Toth PT, Zhang Y, Marsboom G, *et al*. Inhibition of mitochondrial fission prevents cell cycle progression in lung cancer. *FASEB J* 2012; 26: 2175–86.

27   Huang Q, Zhan L, Cao H, Li J, Lyu Y, *et al*. Increased mitochondrial fission promotes autophagy and hepatocellular carcinoma cell survival through the ROS-modulated coordinated regulation of the NFKB and TP53 pathways. *Autophagy* 2016; 12: 999–1014.

28   Zhao J, Zhang J, Yu M, Xie Y, Huang Y, *et al*. Mitochondrial dynamics regulates migration and invasion of breast cancer cells. *Oncogene* 2013; 32: 4814–24.

29   Cassidy-Stone A, Chipuk JE, Ingerman E, Song C, Yoo C, *et al*. Chemical inhibition of the mitochondrial division dynamin reveals its role in Bax/Bak-dependent mitochondrial outer membrane permeabilization. *Dev Cell* 2008; 14: 193–204.

30   Ishihara N, Nomura M, Jofuku A, Kato H, Suzuki SO, *et al*. Mitochondrial fission factor Drp1 is essential for embryonic development and synapse formation in mice. *Nat Cell Biol* 2009; 11: 958–66.

31   Karbowski M, Lee YJ, Gaume B, Jeong SY, Frank S, *et al*. Spatial and temporal association of Bax with mitochondrial fission sites, Drp1, and Mfn2 during apoptosis. *J Cell Biol* 2002; 159: 931–8.

32   Sheridan C, Delivani P, Cullen SP, Martin SJ. Bax-or Bak-induced mitochondrial fission can be uncoupled from cytochrome C release. *Mol Cell* 2008; 31: 570–85.

Supplementary Table 1: Reagents applied in the study.

Reagent or resource	Source	Identifier
Medium		
DMEM	Gibco	Cat#C11965500BT
FBS	Gibco	Cat#10270-106
Penicillin–streptomycin (10 000 U/mL)	Gibco	Cat#15140-122
Keratinocyte SFM	iCell	Cat# iCell-0019
D-(+)-Mannose	Abcam	Cat#ab145352
Commercial assays		
CCK8	Meilunbio	Cat#MA0218-5000
Annexin V-APC/7-AAD Apoptosis Kit	MultiSciences	Cat#AP105
Human Mannose ELISA Kit	ZIKER	Cat#ZK-H594
JC-1 kit	Solarbio	Cat#M8650
Rhodamine 123	MedChemExpress	Cat#HY-D8016
MitoSOX Red	Invitrogen	Cat#M36008
DCFH-DA	Sigma-Aldrich	Cat#D6883
ATP Assay Kit	Beyotime	Cat#S0027
Lipofectamine 3000 Transfection Reagent	Invitrogen	Cat#L3000008
Mito-Tracker Red CMXRos	Beyotime	Cat#C1049
Hoechst 33342	Beyotime	Cat#C1028
IHC kit	MX Biotechnologies	Cat#KIT-9730
Antibodies		
Rabbit anti-MPI	Abcam	Cat#ab154198
Rabbit anti-MFN1	Proteintech	Cat#13798-1-AP
Rabbit anti-MFN2	Proteintech	Cat#12186-1-AP
Rabbit anti-FIS1	Proteintech	Cat#10956-1-AP
Rabbit anti-DRP1	Proteintech	Cat#26187-1-AP
Pro-Apoptosis Bcl-2 Family Antibody Sampler Kit	CST	Cat#9942T
Mouse anti-β-actin	Abcam	Cat#ab8227
Mouse anti-GAPDH	Proteintech	Cat#60004-1-Ig
MODELS		
Prostate cancer tissue microarray (TMA)	Biomax	Cat#PR803d

DMEM: Dulbecco's Modified Eagle Medium; FBS: fetal bovine serum; CCK8: Cell Counting Kit-8; ATP: adenosine triphosphate; IHC: immunohistochemistry; MPI: mannose phosphate isomerase; MFN1: mitofusin 1; DRP1: dynamin-related protein 1; GAPDH: glyceraldehyde-3-phosphate dehydrogenase; TMA: tissue microarray; SFM: serum free medium; Annexin V-APC: Annexin V-allophycocyanin; ELISA: enzyme linked immunosorbent assay; FIS1: fission, mitochondrial 1; CST: Cell Signaling Technology; DCFH-DA: 2,7-dichlorodihydrofluorescein diacetate
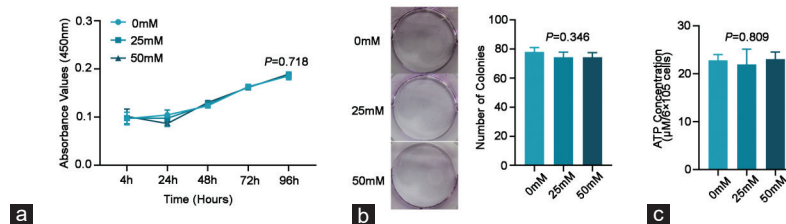
Supplementary Figure 1: The effect of mannose on normal prostatic epithelial cell line RWPE-1. Cell proliferation was assessed using (**a**) growth curves and (**b**) colony formation in RWPE-1. (**c**) The ATP content of RWPE-1 under mannose treatment with multiple concentration.
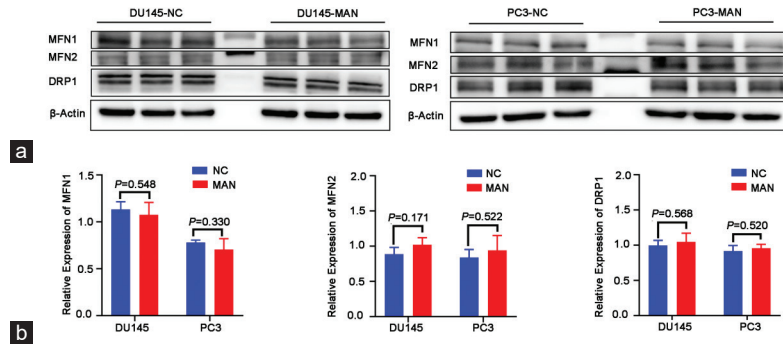
Supplementary Figure 2: The effect of mannose on mitochondrial dynamic related proteins of PCa cells. (**a** and **b**) Western blot was used to measure the expression of MFN1, MFN2, and DRP1 in DU145 and PC3 under mannose treatment. NC: 0 mM. MAN: 25 mM for DU145, 50 mM for PC3. PCa: prostate cancer; MFN1: mitofusin 1; MFN2: mitofusin 2; DRP1: dynamin-related protein 1.
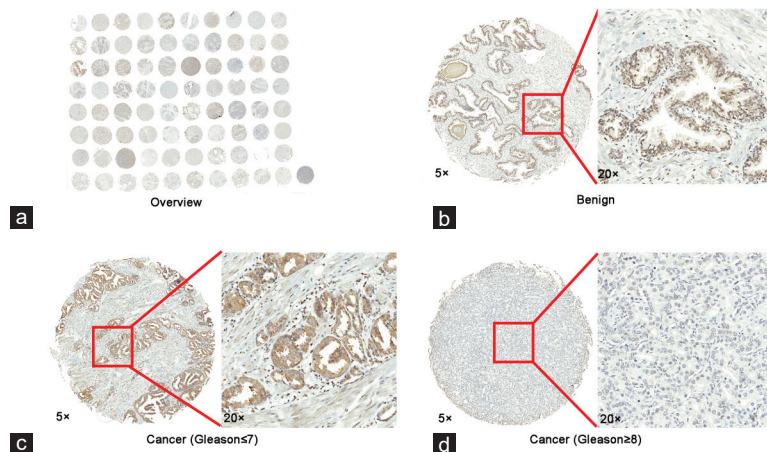
Supplementary Figure 3: Expression of MPI in human prostate cancer tissues. (**a**) Overall view of MPI immunostainings in 80 prostate samples of TMA. (**b–d**) Immunostainings of MPI protein in benign prostate tissues, prostate cancer tissues with low GS (<8), and high GS (≥8), respectively. MPI: mannose phosphate isomerase; TMA: tissue microarray; GS: Gleason score.
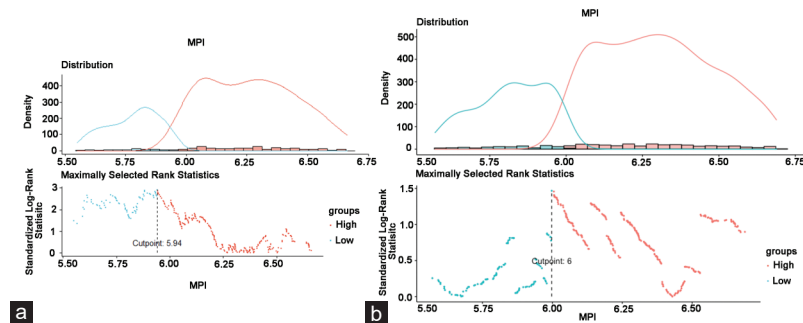
Supplementary Figure 4: The cutoff value of the BCR and overall survival curves. (**a**) The optimal cutoff values of BCR survival curve and (**b**) overall survival curve were determined using the R package "survminer." BCR: biochemical recurrence.